

Dykes, Synclines and Geophysical Inversion – is geology important?

Desmond FitzGerald*

*Intrepid Geophysics
Brighton, Victoria 3186
des@intrepid-geophysics.com*

SUMMARY

In the last 10 years, the average depths of cover for gold and base metal discoveries was 60 and 128 metres respectively (Schodde, 2017). Existing methods of geophysical search techniques appear to lose their practical effectiveness below ~200m. This lack of success has been highlighted as part of the general UNCOVER movement in Australia. A critical and thoughtful response requires not just handwringing, but careful improvements to the whole methodology of exploration geophysics. Clever methods that do not work effectively, can mask this lack of success for a period. The original popularity of the magnetic method is revisited and suggestions are made for what works at depth and what does not. New Airborne ElectroMagnetic 2.5D inversion technology promises to regularly reach to 500m in most terrains, and produce geological sections with marker beds, indicating the local folding and faults.

Key words: Airborne; ElectroMagnetic; 2.5D, Inversion, Exploration; Geophysics

INTRODUCTION

Gunn and Dentith (1997) list a variety of mineral exploration targets associated with magnetic minerals and discuss the use of aeromagnetic methods. This methodology is a good proxy for the traditional interpretation of potential field and other geophysical survey datasets and how they are often still used. With the passing of time, the record for finding deeper buried “orebodies” by direct detection from magnetic datasets, with follow up drilling, has not been very successful. The average depths of cover for gold and base metal discoveries was 60 and 128 m respectively (Schodde, 2017). It is obvious that the “one size does fits all” approach will not work for all mineralization types and mapping the geology remains critical to exploration success. Despite this, the temptation remains that the Tier One deposit that is the only target of interest, has more massive mineralization so hunting the “blob” will work! The experimental evidence indicates this is not so. One malaise that has bedevilled the exploration community has been the over simplistic mantra of drilling the “purple” blob on a magnetic map. A representative list of mineral deposit types is shown in Table 1. This provides a framework to discuss “direct detect” versus “marker bodies” for geological mapping.

In the twenty years since Gunn and Dentith (1997) was published, much change has occurred in the technology space, including desktop computing that far exceeds what could be previously imagined. This has not always been a blessing, as ineffective methods that appear to have merit have emerged and been given much more credence than might have been warranted, if more holistic efforts were made to continue to use other prior geological knowledge.

This paper briefly examines some of the technology advances now available, and attempts an update on the Gunn and Dentith review paper, in the light of the actual performance in the last 10 years of exploration.

- The arrival of computing power that allows for 3D inversions to be made routinely, and to also be used to explore parameter space, means we need to take note of these as well.
- The advent of much more powerful, and sophisticated AEM systems requires that we also make comments about this technology as it can now make a significant addition to exploring for mineral systems.
- The advent of implicit interpolators for mathematically following the rules of structural geology, means we need to take cognizance of this (Calcagno, 2008, FitzGerald 2009).
- Computational geometry engines that are well supported and freely accessible, and capable of describing geological bodies and their intersections, have also emerged e.g. CGAL. CGAL is a software project that provides easy access to efficient and reliable geometric algorithms in the form of a C++ library (<http://www.cgal.org/>).

The form and amplitude of the geophysical responses, such as magnetic or electro-magnetic of a mineral deposit depend on many variables in addition to the concentrations of magnetic, or electrically conductive minerals present. Other key factors are the geometry and depth of the deposit, and its orientation relative to the declination and inclination of the Earth's magnetic field. Survey specifications also come into play, as the sampling of the response is always heavily aliased between lines, compared to along.

What has resisted change, has been the general uptake of measuring gradients and components of potential and electrical fields. The measuring of TMI has now run its full course, and the practical limitations of this signal type as it can be used for exploration, are examined in this paper.

The commonly heard compromise is “give us depth to basement”. This turns out to have many nuances and is not easily achievable using simple methods, in a reliable manner. There are other goals of a simple nature that are nearly as important, that are more reliably achieved, such as define the strike and dip of any contacts where there is a property contrast expression near the surface. Accepting this great reluctance to go to a full 3D inversion, the intermediate steps of deriving elements of a geological interpretation in 3D is examined here. Each proposed element in the output can be critically assessed by an independent geologist, as to its credibility. As with the oil industry, also putting error bars on these new interpretation products or outcomes, looks increasingly vital. Increasing complexity and the explosion of technical data that has developed in our industry, means that robust and smart tools must continue to be developing and offered commercially. These tools must be:

- Readily available,
- dependable, and
- have training material available to demonstrate proper use for their uptake.

METHOD AND RESULTS

Aeromagnetic Grid Data Inversion

Maps of spatial variations in TMI, and products derived from transformations of this primary data type, are typically presented as a grid of values, and are displayed as coloured images. The manual interpretation of magnetic images involves the correlation of observed features and patterns with those expected from the geological environment that comprises the survey area. That is, geoscientific knowledge is used to fit ‘templates’ to the observed responses in what is a subjective interpretational process. The magnetic data may be used to create a pseudo-geological map from which possible sites of mineralization may be inferred based on knowledge and opinion as to what are key controls on deposit formation.

Figure 1, from the Pilbara, Western Australia, is used as the talking point, or Exhibit A for most of this paper. This extract from the WA State grid is compiled by GSWA (Brett, 2016) using the Intrepid Gridmerge tool, with regular updates of newer surveys. Currently the overall grid size is 32 Gigabytes, with a cell resolution of 20m. This chosen area is difficult for any magnetics inversion method, as there is very high remanence on the Northern limbs of the syncline due to alteration, and the residual field reaches 57,000 nT. This is a complex large area with huge amplitudes. Running a quick inversion across this dataset would be a stretch target for most methods. There is clearly a great deal of geological information being captured in the magnetic image. Are we dealing with dykes, a syncline, an anticline, a dome and complex faulting and folding?

Edge Detection for geology structures

Both magnetic and gravity data, processed into a gridded form, are very often subjected to a “Worming” analysis. This is a detection of responses from edges or discontinuities that are associated with structures such as faults, dykes or lithological boundaries (Blakely and Simpson, 1986; Cella et al., 2009; Fedi, 2002). The Intrepid WormE tool is one of the only commercially available implementations. The algorithm has been upgraded to start producing 3D contact surfaces, by the addition of a strike/dip calculation and use of the implicit interpolation methods. This technique can easily find all the anomaly primary edges and trends in Exhibit A. Over 6200 surface 2D segments are produced. A further 50 3D candidate fault/contact surfaces are produced and exported as VTK format files. The dip calculation for these surfaces is purely empirical, as the proper theoretical work remains unfinished for TMI grids. The extension to 3D is also incomplete for magnetics, but complete for standard gravity and FTG. The magnetic tensor can also be used for this analysis. Elapsed time for this exercise is less than 1 hour on a laptop.

These results are in Figure 2 A & B. The different colours in Figure 2A are derived from the strength of the horizontal magnetic gradient anomaly. The majority of the gradients are low (yellow). The highest gradients are blue, and often occur on the Northern arms of the synclines. Both arms of the synclines have much stronger gradients, due to the magnetite content, compared to other indicated linear geology features.

The extension of the method to include 3D representations is shown in Figure 2B. The first element of this is to note the results are being displayed using the DEM to give the topography some context. Then estimates of dip and strike are used to propose local planar features that plunge away from the surface (Work in Progress).

Lazy Inversion for Blobs, or a property only inversion

The most popular methods for geophysicists are the uncomplicated cases where a simple survey for magnetics will show a bulls-eye. Quantifying these anomalies as to volume and depth, even if a very poor realization, is also popular, and we call that “Lazy Inversion”. Drawing from the Table 1 list, the most likely examples of using magnetic inversions for direct detection are -

Case A: Massive nickel sulphide mineralization but not always, as shown in the accompanying caveat in Figure 2B. Case C: Alteration from porphyry-style mineralization where extensive areas of hydrothermal alteration often have different magnetic properties to the areas of unaltered geology.

Case G: Potentially diamondiferous kimberlites, especially in Canada.

Thus, at best, half of the scenarios for large scale orebodies may give a direct detect response to magnetic surveys. This leaves most exploration scenarios requiring an engagement with geological mapping, including comprehensive geophysics, as part of the primary targeting method.

It is normal when using a magnetic grid based 3D inversion to assume an homogeneous mineral body with a magnetic response, and a background host rock with little magnetic character.

In the case of Exhibit A, this already causes many issues, as clearly there are many formations with diverse responses. Inversion using Exhibit A causes a great deal of trouble at the 20 m resolution (basically impossible). To demonstrate the main character of this inversion technique, a resolution of 400 m for the region was used.

When doing these larger inversions, one needs to do a regional inversion first. Getting the regional trend removal is important followed by the compression Vs model cell size ratio. If one compresses the model sensitivity matrix

- too much it gets high internal sensitivity error.
- not enough and the size of the sensitivity matrix explodes to be unmanageable.

Regional TMI

A regional inversion study was run using a 400x400x200 cell matrix and a compression factor of 0.05. Giving a sensitivity matrix (the most important part of the inversion) size of about 6 Gigabytes. Solving for the sensitivity matrix, is the most time-consuming aspect of this technology. A more compressed sensitivity matrix leads to higher errors in the fit. Two further refinements were then quickly trialed. Forming a sensitivity matrix allows the user to create a starting model that locally can fit the observed, while accommodating larger variability. Figure 3A summarizes the use of TMI data to create a model that can in turn, reproduce the observed data. The Test of this model is initially the right hand side plots, where one would expect the miss-fit plots to show noise and no geology. In this regard, even before the predicted model is looked at for being geologically reasonable, there is a failure to reproduce the observed signal.

Vector Magnetic Inversion VRMI

Given the above discussion a VRMI inversion was undertaken (MacLeod & Ellis 2013). This recasts the TMI into vector magnetics components, and allows the magnetic vector to change direction, rather than assuming a constant IGRF inducing field direction—it converged significantly better. Once a vector magnetics assumption is taken into account (Figure 3B), the property inversion starts to show a reduced error misfit with the observed magnetics. The next step is then to take the predicted property distribution from this inversion and compare this to the known syncline – see below.

The work for this study was down-sampled to 400 m magnetic grid resolution, so that each of the 3 runs undertaken, was completed a day at a time. At this resolution, 100 cores were used for 6 hours.

High Resolution Detail Study

It has been estimated that to do a high-resolution 3D UBC style inversion, say at 80 m cell size, on this study area, would take 100 CPU cores, 3 weeks, per run, and would involve the original regional, coarse run, as reported here, followed by many smaller tiles. Normally when there is a good regional, it is followed with a tiling process where there is a set of refined model spaces encapsulated within the regional model space (i.e. not in isolation). The way the algorithm works is it calculates the null space model response of the tile with respect to the regional model and then does the inversion—one needs to be able to hold both sensitivity matrices in memory (normally 12 to 15 Gb).

Aeromagnetic Line Data Inversion

We now discuss updates to one of the original line based inversion methods, and report on some innovations. The line data for this area, from publicly available data, comes from the Geoscience Australia GADDS site. This is powered by the Intrepid Jetstream product, and regularly provides the broader community with more than 90 Terabytes of downloads each year. Line surveys cover some of the chosen zone, they are not uniformly of high quality –

- GSWA_South_Pilbara_Magnetic_Line_data (P1134, from GADDS, poorly levelled with lags, but 200 m)
- GSWA_Ashburton_magnetic_line_data (P1233)
- Hamersley_Basin_(Mt_Phillips_Mt_egerton_Collier_Wyloo) (P513 GA dataset, 1 km line spacing)
- Hamersley Basin East (P509, 2 km spacing, 1993)

The grids from these surveys, plus any additional company contributed data are included in the high quality, high resolution grid, that is managed by GSWA.

The principal reasons for using a line based inversion method are –

- To focus on where there is the most measured signal.
- Grids are low pass filtered, losing more than 80% of the higher frequency content in the process.
- Possible to recover estimates of dips, strike, thickness, susceptibility along narrow bodies etc.

- Stacking line based inversions in a 3D context, allows the inference of main features between lines.
- Allows for a 2.5D method to be used, employing limited strike length 2D model's induced response from the Earth's field.

A scalar grid of the field, while pleasing to the eye, and introducing the interpreter to the main regional features, has much less signal content to work with when details are sought about narrow features.

Naudy (1971) developed an automatic depth estimation routine for application to magnetic profile data based on splitting anomalies into symmetric and antisymmetric components and the subsequent matching of the symmetrical component to the magnetic anomalies of standard simple geometrical forms such as dyke, contact and thin plate models. Refinements to the method have been made by Shi (1991, 1994) who uses horizontal and vertical components of the magnetic field, and added an extension for vertical gradient data.

Extensions to the Naudy methodology include:

- Strike of Anomalies - an automated method to pre-compute the local magnetic trend direction,
- Optimisation of the computation - progressively larger 'depth' steps, and adaptive sub-sampling of the TMI profile data for the deeper computations,
- Forward Modelling & Inversion - Automatic 2.5D modelling, for improvement of solutions by inversion,
- Efficient new facet modelling formulations, involving a skeleton representation, with a local scalar thickness variable. (Mainly to support Tensor magnetic gradients.)
- Non-admissible dyke geometry filtering, for rejection of untenable solutions,
- Clustering, to reduce the individual solutions to continuous "dyke worms", with variable thickness, dip, and susceptibility.
- Implicit function interpolation, based upon the Potential Field technology, Calcagno, 2008, is then used to create limited extent, dyke swarms as 3D closed volumes are computed.

Experience with this new methodology has shown that including body strike significantly improves the quality of computed Naudy solutions, with a greater number of computed bodies producing 'good matches' when model data are matched to field data. Furthermore, the trend data are a useful aid to interpretation of potential field data.

In the study area, at least 4 separate aero-magnetic surveys have been levelled, gridded, then grid merged to form the high resolution, base line magnetic grid, as shown in Figure 1. The P513 dataset is chosen as the demonstrator for this technique. The whole line dataset can be inverted for "dyke" features in approximately one hour on a standard laptop.

Figure 6 shows a screenshot from an interactive session with this tool, capturing Line 110, after a 2D inversion, looking for sloping thin dykes to explain the observed magnetics. In this case, it is known we are dealing with a syncline, but superficially, the surface expression of most of the magnetic signature, looks like a "dyke" i.e. long thin bodies on each arm of the syncline. The aim of an inversion like this is to get some idea of consistency in strike/dip estimations as well as best fit susceptibility distributions on the surface. A total of 490 3D dyke bodies, expressed as linked HOT SPOT related determinations of a "dyke" are written to file.

Aero-Electro-Magnetic Line Data Inversion

In a similar argument to the above concerning line based inversions, the rise of 2.5D AEM inversion for full surveys, is likely to become the general practice, now that the precedent for being able to do this routinely has been set (FitzGerald et al., 2009, Silic 2016). It has taken more than 10 years of R&D to get to this happy place. A succession of proprietary improvements in matrix inversions and higher powered desktop computers, now means anyone can cheaply and quickly perform a 2.5D AEM inversion on their survey data. Silic (2016) demonstrated the benefits of modelling deeper sources, 2D geology structures being defined by conductive marker beds, clearer definition of dipping faults and synclines instead of false anticline pseudo structures common on 1D inversion. The new product name is MOKSHA.

TEMPEST lines are available over the southern part of the region shown in Figure 1. This case study is reported in more detail in Paterson et al. (2017). Figure 7 shows the result of a number of inversion algorithms for TEMPEST lines 1004801 and 1004901. The new 2.5D inversion technique, now called MOKSHA, (This result is the third in the stack for each line's results) removes ambiguity over the question of anticline vs syncline structures evident in 1D EM inversions. This is a very common issue with 1D AEM inversion, as this method is not capable of resolving complex 2D geometry, and so tends to show quite striking "anticlinal features" once the geology is not layer-cake. Prior geological knowledge of the area has this syncline interpreted at depths of up to 5 km.

The proprietary 2.5D inversion algorithm inverts approximately 3 km of data per hour on a high-end desktop. The mineral exploration targets listed in Table 1 are also candidates for a general discussion on detectability for AEM methods. Generally, near surface deposits are more detectable when stimulated with either time or frequency domain primary signals, and induce a secondary response from the more conductive, rather than magnetically susceptible minerals.

For this region, outcropping geology is plentiful with thin, patchy cover, so it is relatively easy to deduce most of the geology by conventional structural mapping. In 2009, Intrepid produced the Brockman Syncline 3D geology model (FitzGerald et al. 2009). In 15 minutes an overview of the main geological features was created from no more than 50 sparse, but representative, field mapping observations. The methods used are described by Calcagno et al., (2008). Timing to create a detailed 3D geology model, by a series of

rebuilding and improvements is around 1 week, as each of the factors is reconciled. Around 40 instances of an improving 3D geology model were used.

Litho-constrained Stochastic Inversion

In the context of this review paper, the inversion of the aero-magnetic data, constrained by a prior geology model, is also reported. The Northern arms of the syncline have had significant alteration which shows up as demagnetizing and weathering effects and/or remanent magnetization.

The stochastic inversion allows for estimates of the remanence magnetic vectors to be solved, in terms of most likely, or a prior property distribution, and then to also have most probable vectors of magnetization estimated at all cells in the 3D model. This is not a trivial job, and took several months of work, to firstly derive reasonable starting properties for each of the rock units, then to use both forward modelling and inversion, to test these properties, and adjust, re-run etc. As work of this nature is at the current limit of technology, and not commonly performed, the proposed bulk rock magnetic properties are presented as typical of a work in progress, rather than substantiated facts. The reliability of the calculated property means and standard distributions depends upon a geology model that is close to reality. As we are largely dealing with magnetic susceptibility in this study, a Log Normal distribution has been chosen. Figure 9 reports a comprehensive table of magnetic property distributions for each formation.

The stochastic inversion misfits for magnetics are always quite small, once the starting geology model captures and explains most of the gravity and magnetics responses. The changes in geometry as well as properties are controlled by the allowable Probability Distributions that have been set for each property/formation in the run. One of the deliverable outcomes from stochastic inversion can also be a property voxel in 3D. This model can be compared directly to the distribution proposed by the UBC technology allowing the creation of a property variance model in 3D by simply recording the differences in space, and fitting an experimental variogram to these values. Of course, the constraints imposed by the requirement to respect the geology model, immediately means that this aspect cannot be captured in the unconstrained case, and so this represents the main difference between this stochastic result and the deterministic method. That is, the stochastic inversion is mostly constrained to honour the prior geology geometry, and the deterministic method has no geometry constraint at all.

Deterministic property Inversion vs Geology Model

Lastly, to bring disparate parts of all this work together, 3D geology models both at the regional scale, and at the Brockman syncline scale (20km) are used to then incorporate all the different deliverable outcomes from the geophysics methods e.g. worms, fault planes, dyke geometries, property voxets (3D regular grid). Any amount of slicing and dicing of the 3D information can then be undertaken to review how each method may or may not have contributed something useful in terms of the geometry of the syncline, and then in turn to the definition of a mineral resource, which is part of the geological entity.

Following Figure 10, parts a,b,c and d shows one of the fundamental issues we all face, in the endeavor to join geology and geophysics. The inherent ambiguity in an unconstrained TMI inversion, means that a mathematical extra constraint, in this case a depth weighting, can result in exaggerating the depth extent of the magnetic bodies proposed to explain the observed signal. At the regional scale, the inversion result generally fails to follow the known syncline geometry. Even if this geology model is not as close to reality as some would like, it still captures the inherent feature. There has been a low end susceptibility property clip applied to the 3D cells, so those parts of the geology section that are not in any way being seen in the magnetics, can be seen. A top end clip of 3 SI units is also applied. This is for the VRMI version, which showed the least error in plan view, and it does reproduce the original observations well. Clearly the inversion technology is being challenged by this context, with many aspects poorly realized. The known geology and the results from Figure 3, are shown in Figure 10 for a North-South section through the most northern syncline limb, extending West to East (Brockman Syncline). The known geology and the blind UBC style inversion show little correlation with each other.

CONCLUSIONS

In the case of Exhibit A (Figure 1, and J in the Table 1), there are known synclines, and folding in the area. The ability to directly detect the syncline has economic benefits, as the McRae shale, which is the marker bed in the AEM sections, carries high grade hematite. The concept of depth to basement makes little sense in this context, as none of the strata in the part of the geology of interest is flat lying. In this case, the dip of the flanks and the thickness of the syncline, are of interest, and can be ascertained from both the AEM, and with careful use, the dyke fitting methods in the Naudy tool. The ability of any of the geophysics survey methods to resolve details at greater than 500 m depth is also questionable. The error terms become quite large, and so an estimate of these errors should also become more commonly demanded.

An inversion method that more closely creates sections that resemble the geology, or important marker beds that imply aspects of the broader geological trends, is much more useful in many of the mineral exploration contexts than an homogeneous blob, or elongated semi-vertical plugs. The ability to work effectively and efficiently, to deduce the most important aspects of the geological setting, remain important for mineral exploration. Only rarely can one cut corners and still enjoy success at finding an unknown new resource. Relatively simple and quick methods that provide a link back to the local parts of the measured or observed line data, and are thus auditable are to be preferred. What needs to be said again, is that advancing geological understanding remains vital to getting the best outcomes from any geophysics surveys conducted to throw light on the resources under cover.

Early stage geophysical inversions should concentrate on showing the geology, rather than the orebody. These early stage inversion methods can be relatively easily achieved, with execution times ranging from an hour to a week. Based upon the work reported in this study, the question of dyke vs syncline vs blob as a starting point for a geological interpretation is almost the wrong question. The prior knowledge of what is the dominant geological setting should be brought to bear, in choosing what geophysics methods to

use to help constrain the suspected or known geological structures. Exploring under cover for minerals in most situations, still requires an evolving understanding of the geological setting. The presentation and use of a 20 m TMI grid of the magnetic field, derived from a combination of 200 m, 1 km, and 2 km line spacing surveys ends up not being that useful in any of the geophysical inversion attempts, and masks the lack of real high frequency local content. The reason for this is that there is an illusion of measured frequencies, constrained by the minimum curvature constraints, but no actual high frequency information that can contribute to the local geological fabric, or interpretations, either by simpler methods or full 3D inversion. It is not so easy to extend the original table prepared by Gunn, to include AEM responses, and the new disciplines of magnetic and gravity gradiometry. This work remains for future papers.

Predictions of Future Technology developments

The interpretation of TMI data, both in its original lines, or a gridded form, no matter how high the resolution of the field, does not allow or give an interpreting geoscientist enough local information in its inherent signal to reduce the ambiguities under cover. Both AEM and magnetic surveying will switch to Full Tensor gradiometry observations. The magnetic tensor gradient surveying business will be first. General commercial availability has been a constraint to the uptake. Tensor AEM is still constrained by a level of complexity at the edge of what can be successfully engineered. Since 2006 the enabling software technology for tensor data processing has been available, with the exception of aircraft compensation for maneuver noise. The digital revolution and material science advances means the sensors required also now exist. It would appear that Chinese innovation might start to get ahead on this aspect, unless Australian Government agencies finally decide to take a risk and promote a demonstration project, using the available German technology.

Everyone, including Government, are constrained by how much they can spend on surveys. From a regional perspective, do you go for large area coverage or small area detail? The false economy of choosing a cheaper survey technique that does not yield more specific detail under cover, is one of the major stumbling blocks. This study shows the inherent limitation of TMI, and the various attempts to try and compensate with software, for the shortcoming of the signal content. Software techniques and computing capacity far exceed the current uptake in the mineral exploration community, which is still stuck in the “looking good on paper” mode of operation. Also, the often-heard comment of claiming “the gradients can be calculated so why measure them?”, must be put to bed once and for all. There are so many compromises with the calculation of full tensor gradient from a scalar measure such as TMI that the errors and the high frequency required are just not tractable. Most geophysics interpretation methods rely on estimating the local gradients of the field. This includes all the methods used in this paper. Measured gradients, even with higher component errors, are better than partial, or scalar measures every time. There are still no published case studies on this subject. One internal study comes to mind for Rio, where the question of measuring one tensor gradient more accurately was compared to measuring all the components less accurately.

In this paper, the demonstration of creating a 3D geology model, using geology gradients and geo-statistics was not spelt out, but this is at the core of that demonstration. It has been shown that a geology gradient measure influences the overall outcome 100 times more powerfully, than any individual scalar measure of a geology contact. It remains a challenge to similarly demonstrate the same outcome for potential field geophysics. This powerful lesson has not been accepted and absorbed by the geoscience community yet.

ACKNOWLEDGMENTS

I thank Peter Gunn for permission to appropriate any/all of his previous musings on this subject and his comments.

REFERENCES

- Brett, JW 2016, 20 m magnetic merged grid of Western Australia 2016 version 1: Geological Survey of Western Australia, Perth.
- Calcagno, P, Chilès, JP, Courrioux, G, Guillen, A, 2008. Geological modelling from field data and geological knowledge, Part1, Modelling method coupling 3D potential field interpolation and geological rules, Physics of the Earth and Planetary Interiors. doi:10.1016/j.pepi.2008.06.013.
- FitzGerald, D, Chilès, J-P, Guillen, A, 2009. Delineate 3D Iron Ore Geology and Resource Models Using The Potential Field Method, Proceedings AusIMM Iron Ore Conference.
- Gunn, P.J., Dentith, M.C., 1997. Magnetic responses associated with mineral deposits. AGSO Journal of Australian Geology and Geophysics 17, 145–158
- MacLeod, I., Ellis, R. 2013, Magnetic Vector Inversion, a simple approach to the challenge of varying direction of rock magnetization, ASEG-PESA-AIG 23th Geophysical Conference and Exhibition.
- Naudy, H., 1971. Geophysics, 36, 717-722.
- Paterson, R., Silic, J., FitzGerald, D, Jakica, S, 2017. High Accuracy 2.5D AEM Inversion Method for Banded Iron Formation (BIF) and Other Geological Settings, SAGA, 2017, Capetown
- Schodde, R, 2017, AMIRA Exploration Managers Conference, Healesville, Victoria, Australia

Shi, Z., 1991. Exploration Geophysics, 22, 357-362.

Shi, Z. & Boyd, D., 1994. Exploration Geophysics, 24, 789-794

Silic, J, Paterson, R, FitzGerald, D, 2016. Improved Structural Mapping and Conductive Targeting Delivered by a new 2.5D AEM Inversion Solver, ASEG-PESA-AIG 25th Geophysical Conference and Exhibition.

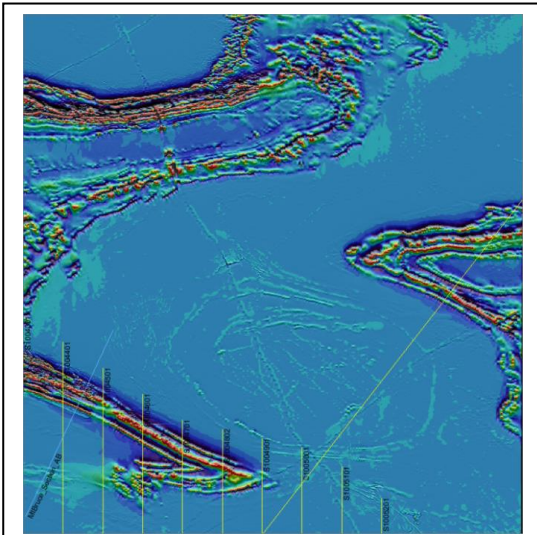


Figure 1. Reduced to Pole First Vertical Derivative TMI draped on Reduced to Pole TMI showing the Brockman and Hardey Synclines and the inverted Tempest AEM flight line paths (yellow lines). Note, reduction to the pole may not work very well where anomalies get up to 57000 nT! Spatial extent is a nominal 90km

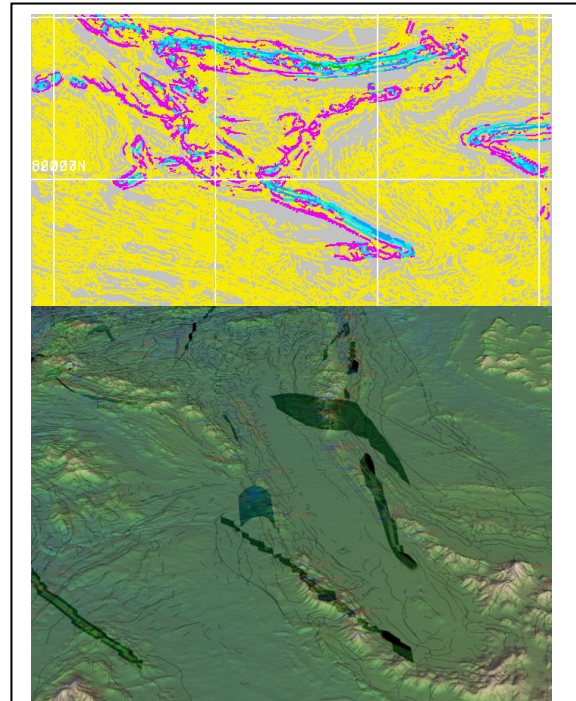


Figure 2. Top (A) shows the classic edge detection results, coloured by horizontal gradient signal amplitude. Bottom (B) is a new extension, combining the DEM with the “worms”, and a start made on 3D surfaces from calculations of the local strike and dip of the contacts. The relationship between topography, weathering and geophysics responses comes into focus as a 3D method is employed.

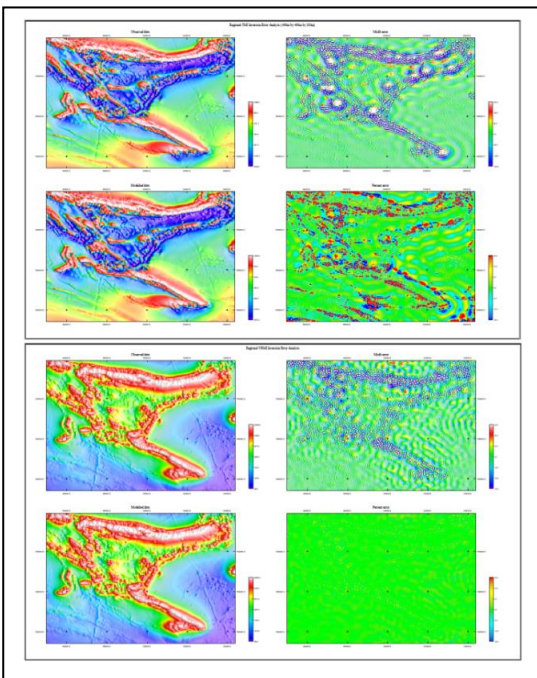


Figure 3. UBC style inversions of the Figure 1 Aero magnetic grid dataset. Left hand plots shows measured then modelled response from the inversion result. The right hand plots show misfits. The top 4 plots, (3A) record a TMI analysis at a regional scale, down sampled to 400 m * 400m, 400 m * 200 m. The lower 4 plots (3B) shows the same data, but now reduced to a Vector Magnetics, or VRMI analysis. For this area with very high non-induced effects, this later step is mandatory in even getting close to a low mis-fit for the inverted property distribution in 3D. The lazy inversion of TMI for this dataset is a clear failure, to even fit the observed.

Type	Common Tag	General Description	Minerals	Magnetic Response
A	VMS	Massive sulphid deposits	Cu,Zn,Pb, Ag,Au	5 types, depending upon orientation, erosion state, tilt: Figure 4 a & b

B	Magnetite-rich	Fe oxides, rather than sulphides	Cu-Au-Bi	bull's-eye magnet anomalies caused by high magnet concentrations
C	Porphyry copper	intrusive felsic porphyritic stocks	Cu, Cu-A-and Cu Mo	semi-pre-dictable magnetic response
D	Skarn Deposits	coarse-grained Ca-Fe Mg-Mn silicates	S-Fe, Cu, W, Zr Pb, Ag	magnetics can aid skarn recognition; the technique cannot be relied upon for the recognition of skarn-hosted mineral deposits
E	Placer	concentrated in palaeodrainage systems	gold, tin, platinum heavy mineral sands, diamonds	
F	Carbonatite		niobium, phosphate rare-earth elements, titanium, fluorite vermiculite	magnetic zoning will be concentric
G	Diamonds	kimberlite and lamproite pipes	Diamonds	Not all kimberlites and lamproites are magnetic clusters of intrusions can include magnetic, non-magnetic and reversely magnetised pipes. A NULL gradient magnetic tensor response has now been recognized.
H	Chrome platinoids	ultramafic intrusions	platinum magnetite and	Koensberger ratios are generally greater than unity, with a maximum of nine.
I	Gold	wide range of geological environments	Au	magnetic data used as a mapping tool
J	Iron Ore		Fe	magnetite or hematite ? hematite ore has a minor response, BIF is strongly magnetic
K	Nickel	nickeliferous laterite, nickel sulphides	Ni	deposits occur in association with basic to ultrabasic (meta)igneous rocks; such rocks tend to have strong magnetic responses. The presence of pyrrhotite and magnetite in many nickel sulphide deposits means that the mineralisation itself may be detectable by the magnetic method. Magnetic data alone are unreliable for locating ore bodies

Table 1 After Gunn and Dentith, 1997. In all cases, the measure of a magnetic field's components, or better the full tensor gradients, would significantly improve the interpretability of the induced and remanent response

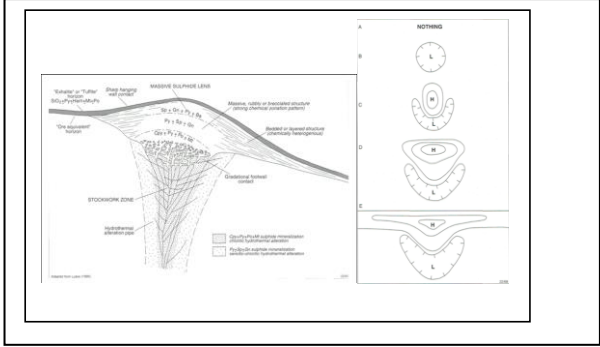


Figure 4. Idealized vertical cross-section of a massive sulphide deposit. Normally, the deposit would have circular symmetry in plan view. If the deposit has been localized by a fault, only one-half of the deposit as shown may occur. Not all the zones illustrated always occur in a single deposit. Figure 4b shows the range of magnetic responses for VMS deposits ranging from nothing (A) to (E), magnetic minerals occur throughout the deposit.

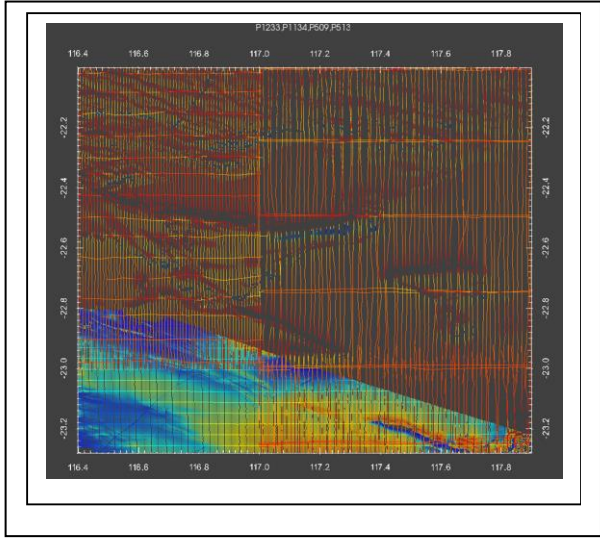


Figure 5 View of the original line data, showing the older surveys plus the difference in the residual levels between GA data and GSWA of around 5000 nT. P513 is the top left hand survey.

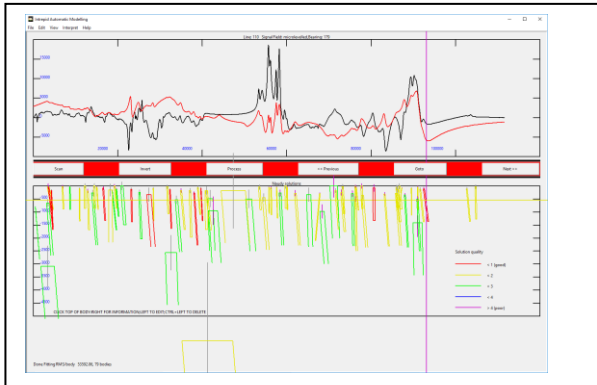


Figure 6. Shows the line based inversion process, for Line 110, of the Geoscience Australia dataset, P513. This is a 1 km line spacing, older dataset, to the Western edge of the study area. Candidate “dykes” are found on each cross-section, then automatically joined to worms, with estimates of susceptibility, thickness, height, after a 2D inversion to improve the fit and estimate a local RMS error.

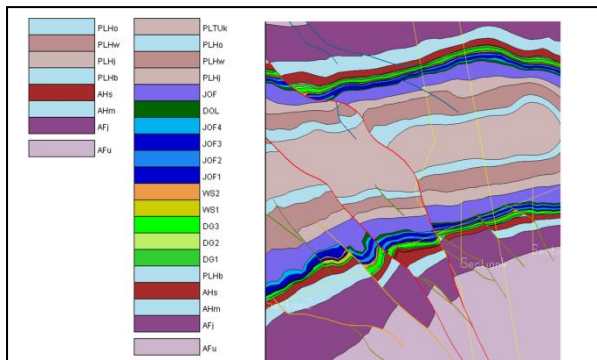


Figure 8. Regional Brockman 4 Syncline model, including the primary faults, and a central fold axis running West-East, with district, derived from a combination of reviewing existing published work, and property optimization using observed magnetic and gravity data. Spatial extent is a nominal 20km.

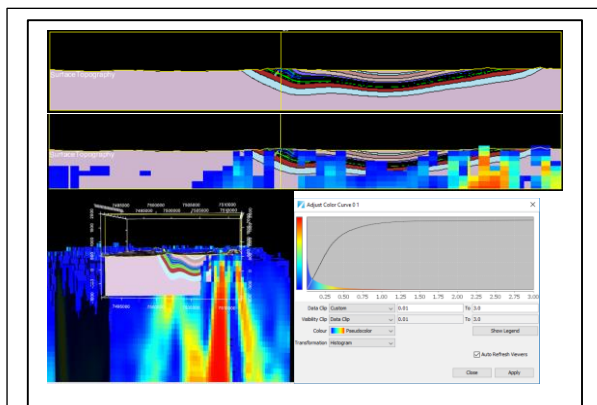


Figure 10 Juxtaposition of the VRMI inversion for susceptibility with depth, beside the 3D geology model of the syncline. Top figure a, the solid model section, Part b, the same but overlain on section with the clipped (> 0.01 SI) susceptibility estimates, Part c, the 3D perspective, with a 4 to 1 vertical exaggeration. The tendency for the inversion to place most of the magnetization at great depth is very clearly shown. A kind interpretation might link the magnetization from the left and right arms of the syncline. Part d, is the colour lookup, with clipping values shown. Lable a,b,c,d in the diagram

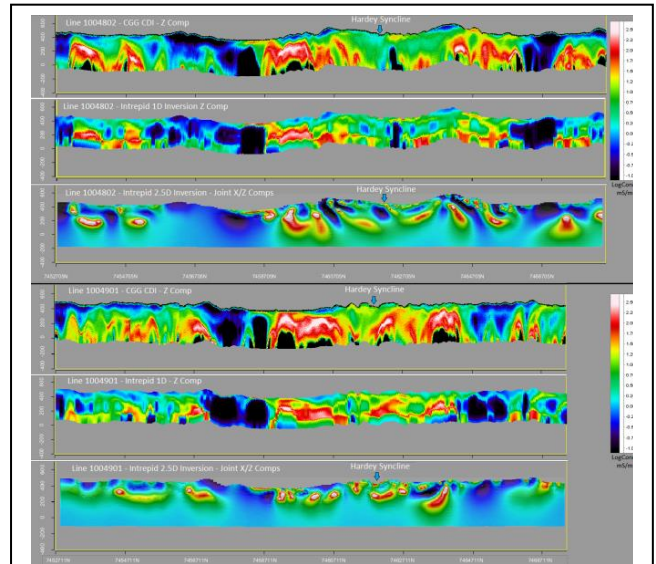


Figure 7. A Comparison of the CGG CDI (Z Comp.) and Intrepid1D (Z Comp.) & 2.5D Inversion (X and Z Comp.) for Capricorn Tempest Line Segments, 1004801 (top 3) and 1004901 (bottom 3) over the Hardy Syncline. Only the 2.5D inversion result shows the syncline in any convincing manner. The inverted crescent moon is positioned below the indicated syncline response. Depth of investigation for the AEM in this case is around 500 m below surface.

Physical Properties		
Formation	Susceptibility (SI)	Remanent Magnetization (A/m)
PLTuk	Log-normal(0.0022,0.0004,100)	Normal(0,0,100,0,0)
PLHo	Log-normal(0.0036,0.0018,30) + Log-normal(0.3635,0.18,70)	Log-normal(0.06,0.03,30,-40,-30) + Log-normal(1.62,0.6,70,-3...
PLHw	Log-normal(0.0039,0.002,100)	Log-normal(0.1,0.01,100,-20,-50)
PLHj	Log-normal(0.0352,0.0214,20) + Log-normal(0.5361,0.2849,80)	Log-normal(0.616,0.3,20,16,20) + Log-normal(2.954,0.3,80,-2...
JOF	Log-normal(0.0319,0.023,20) + Log-normal(0.4225,0.2866,80)	Log-normal(0.356,0.12,100,27,13)
DOL	Log-normal(0.0623,0.0612,100)	Log-normal(0.1,0.01,100,-19,-26)
JOF4	Log-normal(0.0319,0.023,20) + Log-normal(0.4225,0.2866,80)	Log-normal(0.294,0.12,100,51,7)
JOF3	Log-normal(0.0319,0.023,20) + Log-normal(0.4225,0.2866,80)	Log-normal(0.735,0.3,100,-12,61)
JOF2	Log-normal(0.0319,0.023,20) + Log-normal(0.4225,0.2866,80)	Log-normal(0.147,0.07,100,-22,-52)
JOF1	Log-normal(0.0319,0.023,20) + Log-normal(0.4225,0.2866,80)	Log-normal(0.356,0.12,100,27,13)
WS2	Log-normal(0.0319,0.023,15) + Log-normal(0.4225,0.2866,85)	Log-normal(0.8,0.2,100,47,-60)
WS1	Log-normal(0.0319,0.023,15) + Log-normal(0.4225,0.2866,85)	Log-normal(0.8,0.2,100,47,-60)
DG3	Log-normal(0.0319,0.023,20) + Log-normal(0.4225,0.2866,80)	Log-normal(0.298,0.1,100,7,-77)
DG2	Log-normal(0.0319,0.023,20) + Log-normal(0.4225,0.2866,80)	Log-normal(0.298,0.1,100,7,-77)
DG1	Log-normal(0.0319,0.023,20) + Log-normal(0.4225,0.2866,80)	Log-normal(0.298,0.1,100,7,-77)
PLHb	Log-normal(0.0319,0.023,20) + Log-normal(0.4225,0.2866,80)	Log-normal(30,3,100,-11,-13)
AHs	Log-normal(0.0062,0.0032,20) + Log-normal(0.0021,0.0016,80)	Log-normal(0.1,0.01,100,-27,-50)
AHm	Log-normal(0.0103,0.0087,20) + Log-normal(0.497,0.1638,80)	Log-normal(10,0.9,100,-27,-50)
AFj	Log-normal(0.005,0.0008,100)	Log-normal(1,0.1,100,-27,-50)
AFu	Log-normal(0.0054,0.0007,100)	Log-normal(1,0.1,100,-27,-50)
Cover	Normal(0,0,100)	Log-normal(0,0,100,0,0)
Dolerite	Log-normal(0.00623,0.003,100)	Log-normal(0.1,0.01,100,-19,-26)
FWZ	Normal(0,0,100)	Normal(0,0,100,0,0)
NS	Normal(0,0,100)	Normal(0,0,100,0,0)
TD2	Normal(0,0,100)	Normal(0,0,100,0,0)
XX	Normal(0,0,100)	Normal(0,0,100,0,0)

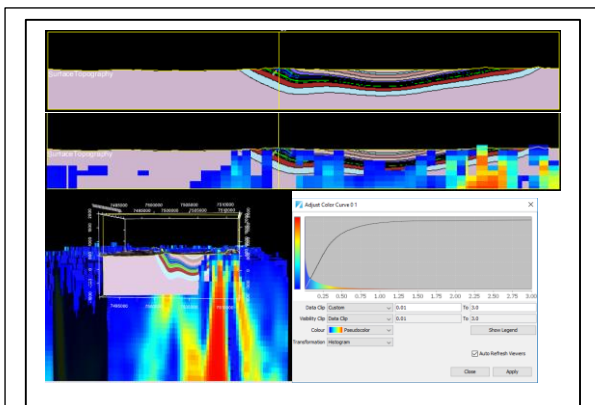


Figure 10 Juxtaposition of the VRMI inversion for susceptibility with depth, beside the 3D geology model of the syncline. Top figure a, the solid model section, Part b, the same but overlain on section with the clipped (> 0.01 SI) susceptibility estimates, Part c, the 3D perspective, with a 4 to 1 vertical exaggeration. The tendency for the inversion to place most of the magnetization at great depth is very clearly shown. A kind interpretation might link the magnetization from the left and right arms of the syncline. Part d, is the colour lookup, with clipping values shown. Lable a,b,c,d in the diagram

Figure 9. Magnetic Properties of the Hammersley Ranges rocks, as deduced from joining the geology model and the observed aeromagnetic data, and then reconciling by property optimization for bulk properties, and stochastic inversion.